

JGR Biogeosciences

RESEARCH ARTICLE

10.1029/2019JG005198

Key Points:

- The transition from deserts to grasslands in northwestern China amounted to $51.54 \times 10^3 \text{ km}^2$ during the period 2000–2015
- The ecosystem functions of forests and grasslands showed an asymmetric response in the southwestern and northwestern regions
- The Loess Plateau and the Three Rivers Source region represent the mostly effectively recovered regions of western China

Supporting Information:

- Supporting Information S1
- Table S1

Correspondence to:

C. Gang,
 gangcc@ms.iswc.ac.cn

Citation:

Gang, C., Gao, X., Peng, S., Chen, M., Guo, L., & Jin, J. (2019). Satellite observations of the recovery of forests and grasslands in western China. *Journal of Geophysical Research: Biogeosciences*, 124, 1905–1922. <https://doi.org/10.1029/2019JG005198>



Received 7 APR 2019

Accepted 9 JUN 2019

Accepted article online 20 JUN 2019

Published online 6 JUL 2019

Satellite Observations of the Recovery of Forests and Grasslands in Western China

Chengcheng Gang^{1,2,3} , Xuerui Gao^{1,2}, Shouzhong Peng^{1,2} , Mingxun Chen⁴, Liang Guo^{1,2}, and Jingwei Jin^{1,2}

¹Institute of Soil and Water Conservation, Northwest A&F University, Yangling, China, ²Institute of Soil and Water Conservation, Chinese Academy of Sciences and Ministry of Water Resources, Yangling, China, ³International Center for Climate and Global Change Research, School of Forestry & Wildlife Sciences, Auburn University, Auburn, AL, USA,

⁴College of Agronomy, Northwest A&F University, Yangling, China

Abstract The “Grain for Green” Program (GGP), which combats and reverses the landscape-scale habitat degradation by converting agricultural lands to forests and grasslands, was launched in 1999 in western China. An assessment of the extent to which the GGP has altered the vegetation cover and ecological functions in these regions is much needed. The present study initially analyzed land use and cover change of forests and grasslands over western China between 2000 and 2015. A variety of satellite-based ecological indicators, including net primary productivity, normalized difference vegetation index, leaf area index, carbon use efficiency, and water use efficiency, were used to reflect the biophysical consequences of the GGP in western China. Results indicated that the spatial extent of forests and grasslands increased by 13.97×10^3 and $11.13 \times 10^3 \text{ km}^2$, respectively, which were mainly converted from deserts and croplands. The ecosystem functions of forests and grasslands showed an asymmetric response in northwestern and southwestern China. The normalized difference vegetation index and water use efficiency of forests, as well as the net primary productivity and water use efficiency of grasslands, increased significantly over this period. The GGP also has led to an increase in leaf area index and carbon use efficiency of forests and grasslands. The Loess Plateau and the Three Rivers Source area represent the most effectively recovered regions in western China. Rising precipitation rates have contributed to vegetation recovery to some extent, especially in northwestern China, whereas the GGP was the prominent reason for the improvement of ecosystem functions across the entire region of western China.

Plain Language Summary Land degradation has caused severe environmental problems in many areas worldwide and severely restrains the sustainable development of numerous local economies. Land degradation also undermines the livelihoods and food security of people, especially in the economically underprivileged regions. Western China has experienced land degradation because of both its geological location and climatic conditions. To combat and mitigate this situation, the Chinese government implemented a series of national-scale ecological policies and programs during the late 1990s and early 2000s. Nearly 20 years have passed since the implementation of these projects. Therefore, it is appropriate to comprehensively assess the biophysical consequences of these programs. The present study aims to evaluate the extent to which the vegetation of western China recovered during the 2000–2015 period based on a variety of remotely sensed data streams. Results indicated that the spatial extent of forests and grasslands have expanded. The ecosystem functions of forests and grasslands showed an asymmetric response in the southwest and northwest regions of western China. These findings may provide guidelines for government agencies and policy makers involved in initiating adaptation strategies designed to adapt to climate change and to manage vegetation production.

1. Introduction

Land degradation, defined as the long-term loss of ecosystem function and productivity caused by disturbances from which land cannot recover independent of human intervention, is a global issue that has caused severe environmental problems (Bai et al., 2008; Barrow, 1991). Land degradation severely restrains the sustainable development of many local economies and undermines the livelihood and food security of people, especially in the economically underprivileged regions (Andersson et al., 2011; Le

et al., 2016). An assessment by the United Nations Food and Agriculture Organization found that $6,140 \times 10^6$ ha of the world's land has been affected by degradation and 26% of this land is severely or very severely degraded (Gibbs & Salmon, 2015). The various causes of land degradation include a drying climate, a rapid increase in human population, soil loss, deforestation, and unbalanced crop and livestock stocking levels (Taddese, 2001). The geographic location of western China makes it relatively prone to land degradation. Northwestern China is dominated by an arid and semiarid climate and includes nearly 90% of China's desertified land. The Loess Plateau, covered by an average depth of 100 m of loess soil, is ranked as the most erodible area in the world (Sun et al., 2015; Zhang & Liu, 2005). In contrast, the climate in the southwest region of western China is relatively favorable for vegetation growth. However, various geological formations, including the mountainous terrain and karst topography, make the southwestern region sensitive to natural disturbance (Li, 2000). Combined with recent intense anthropogenic activity, the entire region of western China has experienced pressing environmental problems since the 1980s.

To combat and mitigate the land degradation, the Chinese government implemented a series of national-scale ecological policies and programs during the late 1990s and early 2000s, including the "Three-North Shelter Forest Program," the "Grain for Green Program" (GGP), and the "Grazing Withdrawal Program" (Mu et al., 2013; Xiao, 2014). The GGP, which aims to produce an increase in vegetation cover by converting croplands and grazing lands to woodlands and grasslands, is the most famous ecological project in human history due to its massive scale, great cost, and potentially enormous impact (Moore et al., 2016; Wang et al., 2007). Numerous studies have been conducted to evaluate the ecological effects of these restoration programs since their implementation. Previous studies have demonstrated that the afforestation resulting from these programs has greatly improved the carbon storage, biomass, and biodiversity in plants and soils in treated areas (Deng et al., 2014, 2017; Zhao et al., 2013). The rapidly growing tree species planted during afforestation contributed significantly to the increase in vegetation cover increase in most treated karst regions (Brandt et al., 2018; Tong et al., 2017). The revegetation led to a decrease of soil erosion in the highly erodible soils of the Loess Plateau, which helped to conserve the soil and water resources across the expansive region (Xiao, 2014; Zhao et al., 2013). Hydrological processes, latent heat fluxes, and land surface albedo have also been altered at regional scales by converting land use patterns from croplands to forests (Xiao, 2014).

The development of remote sensing data provides an alternative method for quantifying the dynamics of changes in vegetation structure and function at broad scales (Chen et al., 2015; Piao et al., 2005; Xiao, 2014; Zhou & Van Rompaey, 2009). The use of Moderate Resolution Imaging Spectroradiometer (MODIS) data is among one of the most widely used observation methods for monitoring the continuous changes in vegetation (Chen et al., 2015; Xiao, 2014; Yuan et al., 2014). Tong et al. (2017) used remote sensing data to reveal that the leaf area index (LAI) and aboveground biomass of vegetation increased in southwestern karst regions of China. The modeling results driven by remote sensing data indicated that net primary productivity (NPP) of vegetation increased in midwestern China in the past decade (Liang et al., 2015). The detection of vegetation trends using MODIS data provides a practical approach for assessing the effectiveness of the Three-North Shelter Forest Program (Lü et al., 2015). However, there has been little evidence on the dynamics of forests and grasslands cover and the subsequent ecological consequences induced by the GGP across the entire region of western China. Nearly 20 years have passed since the implementation of the above mentioned ecological programs. Therefore, it is timely to comprehensively assess the biophysical consequences of these programs in western China.

The present study aims to (i) characterize the land use and cover change (LUCC) of forests and grasslands in western China during the 2000–2015 period; (ii) quantify the characteristics of forests and grasslands based on a variety of remotely sensed data streams, including the normalized difference vegetation index (NDVI), net primary productivity (NPP), leaf area index (LAI), carbon use efficiency (CUE), and water use efficiency (WUE); and (iii) calculate the correlations between these indicators and climatic variables, namely, mean annual temperature (MAT), mean annual precipitation (MAP), and annual solar radiation, to reflect how the functions of vegetation have been affected by environmental factors. The findings of this study illustrate how the natural vegetation has been restored in western China and also provide guidelines for government agencies and policy makers involved in initiating adaptation strategies to respond to climate change and to manage vegetation production.

2. Materials and Methods

2.1. Study Area

The area of western China covers nearly 6.70×10^6 km², occupying about 70% of China's land area, and supporting 28% of China's population (Figure 1). This region consists of six provinces (Shaanxi, Sichuan, Gansu, Qinghai, Yunnan, and Guizhou), five autonomous regions (Ningxia Hui Autonomous Region, Inner Mongolia Autonomous Region, Xinjiang Uygur Autonomous Region, Guangxi Zhuang Autonomous Region, and Tibet Autonomous Region), and one municipality directly under the central government in Beijing (Chongqing).

Western China features a typical continental climate with MAT ranging from -5 to 23 °C and MAP from 30 to 1,800 mm (Liu & Lu, 2009). The northwestern and southwestern regions exhibit distinct climate conditions with rich precipitation and vegetation resources in the southwest but less precipitation and high evaporation rates in the northwest (Brandt et al., 2018; Shi et al., 2007). In addition, the Qinghai-Tibetan Plateau has its own unique type of climate (Ding & Dong, 2002). Croplands, forests, and grasslands dominate the southwestern China, while grasslands and barren land dominate in northwestern China. Based on the land use and land cover data in 2015, grasslands are the most widely distributed vegetation in western China, covering 45.86% of the total land area. The areas of barrens/deserts, croplands, and forests account for 24.95%, 13.44%, and 14.94% of total area of western China, respectively.

2.2. Data Source and Processing

2.2.1. Climate Data

The meteorological data, including monthly average temperature, monthly precipitation, and monthly solar radiation during the period 2000–2015 were used in this study. These data were obtained from the China Meteorological Data Service Center (<http://data.cma.cn/>) and interpolated by using ANUSPLIN (version 4.2) to generate monthly data layers with a spatial resolution of 1,000 m. The spatial distribution of weather stations in western China was shown in supporting information Figure S1.

2.2.2. Land Cover Data

The European Space Agency Climate Change Initiative Land Cover (ESA CCI-LC) maps (<https://www.esa-landcover-cci.org/>) were used in the present study to generate the annual land cover map of western China from 2000–2015. The new CCI-LC maps were established based on Advanced Very High Resolution Radiometer (AVHRR), Système Pour l'Observation de la Terre-VEGETATION (SPOT-VEG), the Medium Resolution Imaging Spectrometer (MERIS), Project for On-Board Autonomy-Vegetation (PROBA-V), and associated metadata. The overall weighted-area accuracy of the global CCI-LC map is of 71.7% (ESA, 2017). These data sets describe the global and consistent geographical distribution of global land cover at a resolution of 300 m, which have been widely used in modeling land-surface and detecting the land use/land cover change worldwide (Kuppel et al., 2017; Li et al., 2018; Yang et al., 2017). This data set includes 14 natural, five developed and mosaic, and three nonvegetated land classes (Bontemps et al., 2015; Duveiller et al., 2018). In the present study, only the forests, grasslands, deserts, and croplands were assessed in monitoring the land use and cover change in western China during the period 2000–2015.

2.2.3. NDVI, Gross Primary Productivity, NPP, LAI, and Evapotranspiration

The MODIS NDVI data (MOD13A3 V006) were used to reflect the vegetation greenness in western China from 2000 to 2015. The MOD13A3 product, which consists of NDVI and enhanced vegetation index at 1.000-m spatial resolution, is generated by using a temporal compositing algorithm of 16-day MODIS output based on a weighted average scheme intervals (<http://www.ntsg.umt.edu/project/modis/default.php>). The NDVI, which is closely correlated with Fraction of Photosynthetically Active Radiation absorbed by vegetation (FPAR), was used to capture the contrast between the visible-red and near-infrared reflectance of vegetation canopies and photosynthetic activity (Liu et al., 2016; Xiao & Moody, 2004). This index has been frequently used in detecting the vegetation recovery in western China (Chen et al., 2015; Feng et al., 2016; Piao et al., 2005; Zhou & Van Rompaey, 2009). In the present study, the Savitzky-Golay smoothing filter was employed to improve the quality of monthly NDVI time series images, then the maximum value composites method was used to generate annual NDVI data from 2000 to 2015 in the western China.

The MODIS gross primary productivity (GPP) and NPP (MOD17A3) were used in this study to demonstrate the vegetation productivity of forests and grasslands (<http://www.ntsg.umt.edu/project/modis/default.php>).

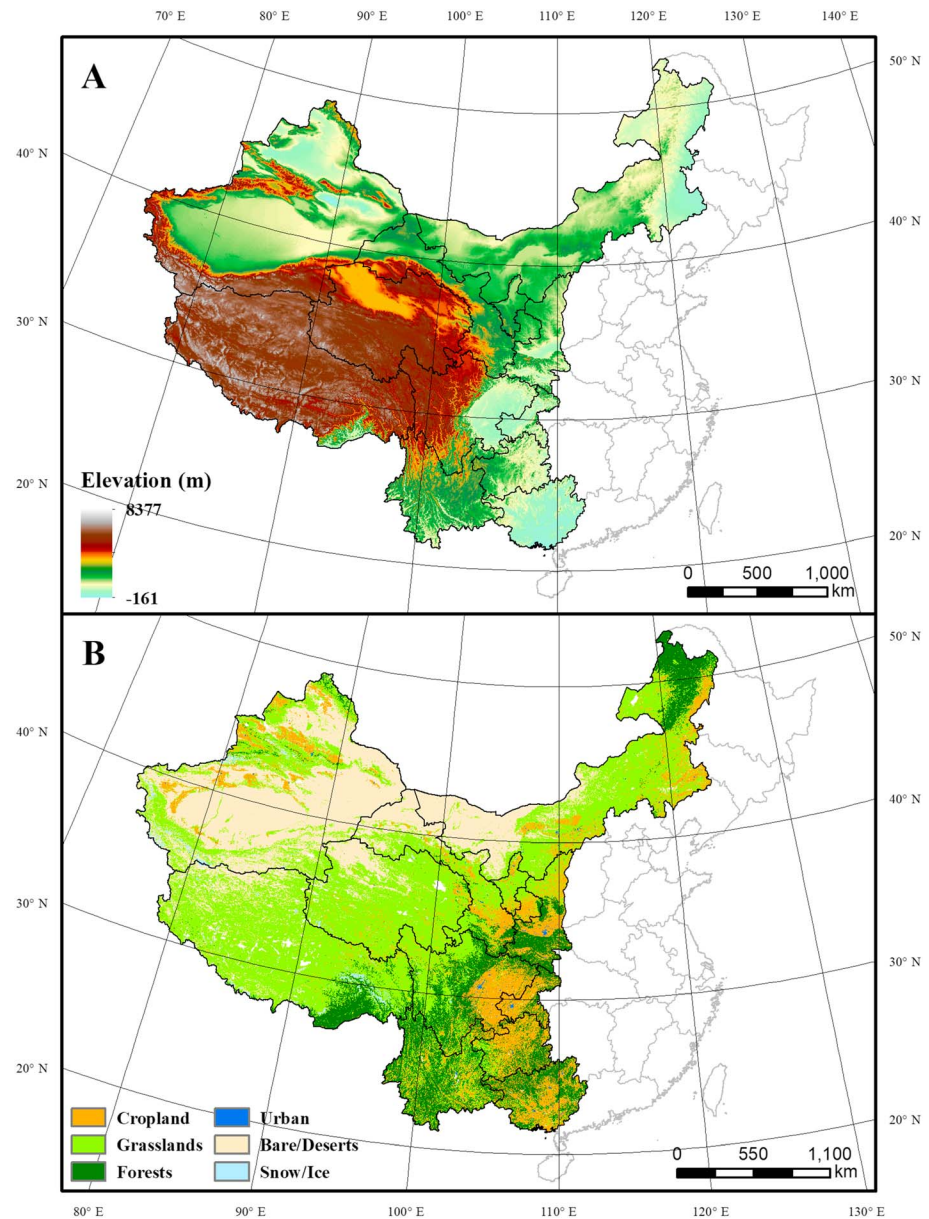


Figure 1. The elevation (a) and land use types (b) of western China in 2015.

The MOD17 algorithm is based on the original solar radiation use efficiency logic of Monteith, which indicates that vegetation productivity under nonstressed conditions is linearly related to the amount of absorbed photosynthetically active radiation (Monteith, 1972). The absorbed photosynthetically active radiation was translated into an actual productivity estimate via a conversion efficiency parameter, ϵ , which is specified by the vegetation type and climate conditions (Running et al., 2004; Zhao et al., 2005, 2006). The ecosystem-scale CUE, the ratio of NPP to GPP, refers to the capacity of a certain ecosystem to transfer carbon from the atmosphere to plants. It has been widely studied to evaluate the ability of vegetation to fix carbon (Dillaway & Kruger, 2014; Gang et al., 2016; Y. Zhang, Yu, et al., 2014).

LAI is defined as one-sided green leaf area per unit of ground area for broadleaf canopies and as the projected needle leaf area for coniferous canopies (Myneni et al., 2002). As one of the most important vegetation parameters used for modeling physical and biological processes, LAI is related to vegetation dynamics and their effects on the global carbon cycle (Deng et al., 2006). In the present study, the GLOBMAP LAIv3 was used to quantify the changes in vegetation LAI in western China during the 2000–2015 period (<http://modis.cn/>).

This annual data set, extending from 1981 to 2017 with 0.08° spatial resolution (~7,000 m), was quantitatively fused by historical AVHRR NDVI data and MODIS land surface reflectance product (Deng et al., 2006). The biome specified clumping index was included in the algorithm calculating the true LAI in GLOBMAP LAI product (He et al., 2018; Liu et al., 2012). The results were validated by global field measurements and fine-resolution LAI maps, and the long-term LAI could explain 71% of variability in the site-based observations covering all major biomes (Liu et al., 2012). The GLOBMAP LAIv3 data set decreased the temporal noise and root-mean-square error by more than 50% when compared with the AVHRR and MODIS data (Liu et al., 2012). Detailed descriptions and evaluations of the algorithm are reported in the paper of Liu et al. (2012).

WUE, the ratio of NPP to evapotranspiration (ET), was used in the present study to address the changes in the water cycles of forests and grasslands. The newly improved version of MODIS ET product recalculates the fraction of vegetation cover, soil heat flux, canopy water loss, soil evaporation, stomatal conductance, aerodynamic resistance, and boundary layer resistance using meteorological data and remote sensing data from MODIS (Mu et al., 2007, 2011).

The annual averaged values of NDVI, NPP, LAI, WUE, and CUE for grasslands and forests were plotted against time separately to show their temporal dynamics between 2000 and 2015. The time series of these annual averaged values were produced based on the land cover map for each year.

2.3. Methods

2.3.1. Mann-Kendall's Test

Mann-Kendall's test, a nonparametric method, was used to assess trends of climate factors (MAP, MAT, and solar radiation) and ecological indicators (NDVI, NPP, LAI, WUE, and CUE). The Man-Kendall's test is superior in detecting time sequential orders for it does not need the data series to be normally distributed. It has been widely used in meteorology, ecology and agriculture research (Liu et al., 2016; Tessema et al., 2011; Xu et al., 2004). The Man-Kendall's test statistics is calculated as

$$S = \sum_{i=1}^{n-1} \sum_{j=i+1}^n \text{sgn}(x_j - x_i) \quad (1)$$

where S is the Mann-Kendal's test statistics; x_i and x_j are the sequential rainfall or temperature values in years i and j ($j > i$) and n is the length of the time series. A negative S value represents a decreasing trend and positive values indicate increasing trends. A test statistic is computed and compared with a critical value at the significance level $p = 0.1, 0.05,$ and 0.01 to decide whether the null hypothesis is accepted or rejected (Kendall, 1948; Mann, 1945).

The Mann-Kendall's test of these indicators was calculated via raster.kendall using the "SpatialEco" package implemented in the RStudio statistical software environment (RStudio Inc., Boston, MA, USA; Yue & Wang, 2002). The uncertainty level of ecological indicators was presented as the width of the confidence interval (i.e., difference between the upper and lower bounds) at a 95% confidence level.

2.3.2. The Partial Correlation Analysis

In evaluating the relationship between climatic factors (MAT, MAP, and solar radiation) and ecological indicators (NDVI, NPP, LAI, WUE, and CUE), the partial correlation analyses was conducted to exclude the confounding effects of other variables. Partial correlation analysis is a widely applied statistical tool to isolate the relationship between two variables from the confounding effects of many correlated variables (Beer et al., 2010; Peng et al., 2013). The Pearson correlation coefficient was firstly calculated as follows:

$$r_{xy} = \frac{\sum_{i=1}^n (x_i - \bar{x})(y_i - \bar{y})}{\sqrt{\sum_{i=1}^n (x_i - \bar{x})^2 \sum_{i=1}^n (y_i - \bar{y})^2}} \quad (2)$$

where r_{xy} is the Pearson coefficient between x and y . x_i is the value of each ecological indicator in the year i , y_i represents the value of climate factors in the year i . \bar{x} is the mean value of ecological indicators over the 16 years, and \bar{y} is the mean value of climate factors over the 16 years. n is the number of years, which is 16 in the

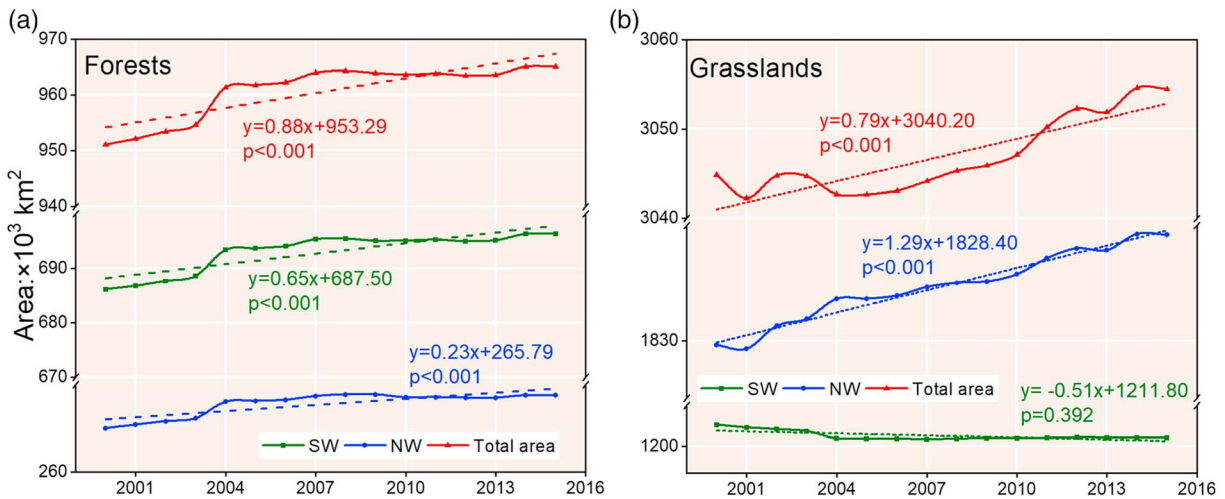


Figure 2. The area dynamic of forest (a) and grassland (b).

present study. For the correlation analysis, all the ecological indicators were aggregated to a 1,000-m spatial resolution to match that of meteorological data.

The partial correlation analysis was determined by the formula

$$r_{12,34} = \frac{r_{12,3} - r_{14,3}r_{24,3}}{\sqrt{(1 - r_{14,3}^2) + (1 - r_{24,3}^2)}} \quad (3)$$

where $r_{12,34}$ means the partial correlation coefficient between variable 1 and 2 when the variables 3 and 4 are fixed. $r_{12,3}$, $r_{14,3}$, $r_{24,3}$, $r_{14,3}$, and $r_{24,3}$ means the partial correlation coefficient between first two variables when the third variable is fixed.

3. Results

3.1. LUCC of Forests and Grasslands in Western China

The results showed that the total area of forests and grasslands both increased from 2000 to 2015 ($p < 0.001$; Figure 2). The total area of forests increased by $13.97 \times 10^3 \text{ km}^2$ over the study period, with 10.20×10^3 and $3.77 \times 10^3 \text{ km}^2$ of the increase occurring in southwestern and northwestern China, respectively. The grasslands area experienced a net increase of $11.13 \times 10^3 \text{ km}^2$ in all of western China over the study period. The grasslands area increased by $19.64 \times 10^3 \text{ km}^2$ in northwestern region; however, it decreased by $8.51 \times 10^3 \text{ km}^2$ in southwestern region. At the provincial level, the smallest and largest increases in forests were observed in Qinghai and Yunnan, which increased by 0.05×10^3 and $6.08 \times 10^3 \text{ km}^2$ during the 2000–2015 period, respectively (Table 1). The only descending trend for forests area occurred in Ningxia ($0.02 \times 10^3 \text{ km}^2$). The smallest increase in the spatial extent of grasslands occurred in Ningxia ($0.26 \times 10^3 \text{ km}^2$) with the largest amount increase in Xinjiang ($7.40 \times 10^3 \text{ km}^2$). A decreasing trend for grasslands was observed in six provinces, in which the smallest and largest decreases occurred in Chongqing ($0.96 \times 10^3 \text{ km}^2$) and Yunnan ($6.85 \times 10^3 \text{ km}^2$), respectively. Overall, the area of both forests and grasslands increased only in Tibet, Gansu, Qinghai, Xinjiang, and Inner Mongolia.

Based on the land use and land cover data in 2000 and 2015, $22.81 \times 10^3 \text{ km}^2$ of forests was converted from other land uses, of which 91.88% was converted from grasslands (Figure 3). Meanwhile, $8.84 \times 10^3 \text{ km}^2$ of forests was transformed into other land uses, of which 71.15% was converted to grasslands. The area of newly developed grasslands amounted to $63.27 \times 10^3 \text{ km}^2$, of which 81.46% were converted from deserts to grasslands. Meanwhile, the total area of grasslands lost was slightly less than the amount of newly developed grasslands. About $52.14 \times 10^3 \text{ km}^2$ of grasslands was changed into other land use types (Table S1). The conversion from grasslands to forests and croplands contributed 40.20% and 31.20% of the loss of original

Table 1

The Area of Main Converted-Out and Newly Developed Land Use Types Between 2000 and 2015 for Each Province (Unit: $\times 10^3 \text{ km}^2$)

Region	Provinces	Converted-out types				Newly developed types		
		Croplands	Grasslands	Forests	Deserts/barren	Croplands	Grasslands	Forests
Northwest region	Inner Mongolia	2.17	11.66	1.50	10.89	5.71	13.50	2.48
	Shaanxi	2.31	1.49	0.20	0.07	0.26	0.45	1.21
	Gansu	0.91	2.43	0.06	5.37	1.16	5.76	0.36
	Qinghai	0.87	2.32	0.01	9.43	1.15	10.16	0.06
	Ningxia	0.13	0.83	0.02	1.06	0.53	1.09	0.00
	Xinjiang	1.97	10.36	0.63	26.61	15.36	17.77	2.08
	Subtotal	8.35	29.08	2.42	53.43	24.16	48.73	6.19
Southwest region	Guangxi	1.67	2.69	2.24	0.00	1.26	1.42	2.64
	Chongqing	1.04	0.99	0.10	0.00	0.10	0.03	1.24
	Sichuan	2.34	4.09	1.21	0.04	1.59	1.24	3.06
	Guizhou	0.45	1.24	0.61	0.00	0.68	0.16	0.83
	Yunnan	1.34	8.41	1.87	0.00	0.64	1.55	7.95
	Xizang	0.94	5.64	0.39	8.96	1.19	10.14	0.92
	Subtotal	7.78	23.06	6.42	9.00	5.47	14.54	16.64
Total area in western China		16.13	52.14	8.84	62.43	29.63	63.27	23.83

grassland, respectively. In summary, the distribution of forests and grasslands both expanded over the 16-year period, with the expansion of forests occurring more extensively than grasslands.

Figure 3 also shows the spatial pattern of LUCC in western China. Geographically, the most obvious variation was the transition from deserts to grasslands, which stretched from the northern Inner Mongolia, spanning Gansu and Qinghai, and extended to Xinjiang. In northwestern China, the intense LUCC was often represented by the transition from barren/deserts to grasslands, where a mosaic region of grasslands, forests,

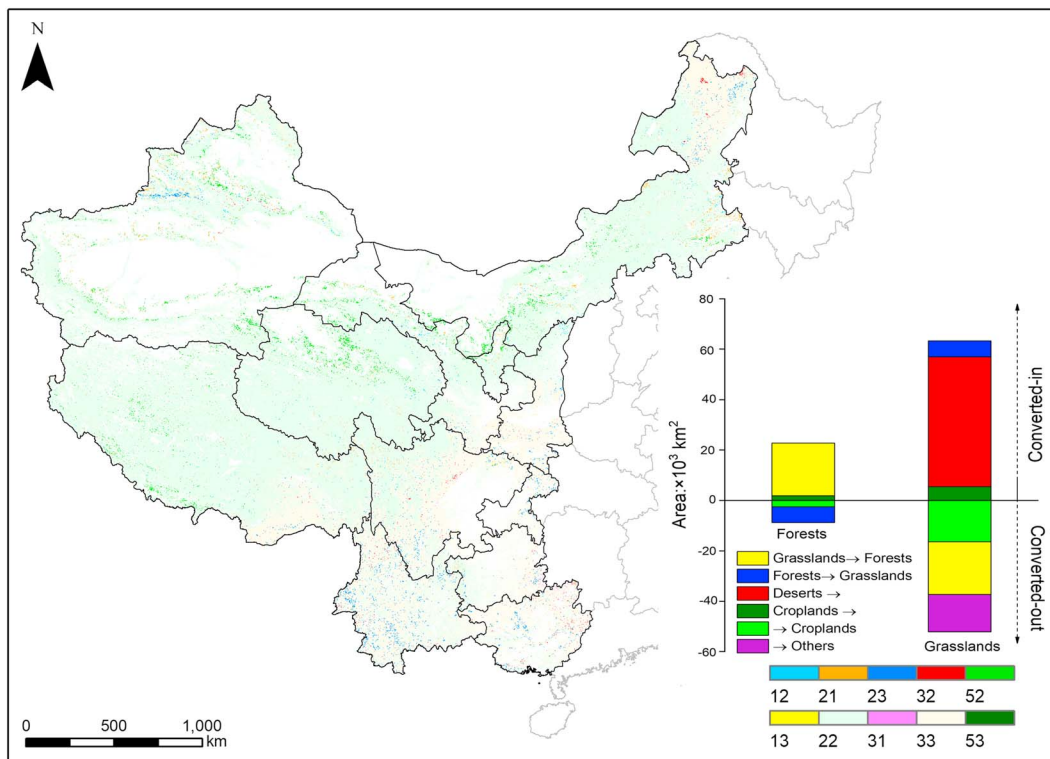


Figure 3. The spatial pattern of main land use changes in western China between 2000 and 2015. 12: grasslands \rightarrow croplands; 21: croplands \rightarrow grasslands; 23: grasslands \rightarrow forests; 32: forests \rightarrow grasslands; 52: barren/deserts \rightarrow grasslands; 13: croplands \rightarrow forests; 31: forest \rightarrow croplands; 53: barren/deserts \rightarrow forests. Numbers 22 and 33 denote the unchanged grasslands and forests, respectively. The map was generated based on the land cover data in 2000 and 2015.

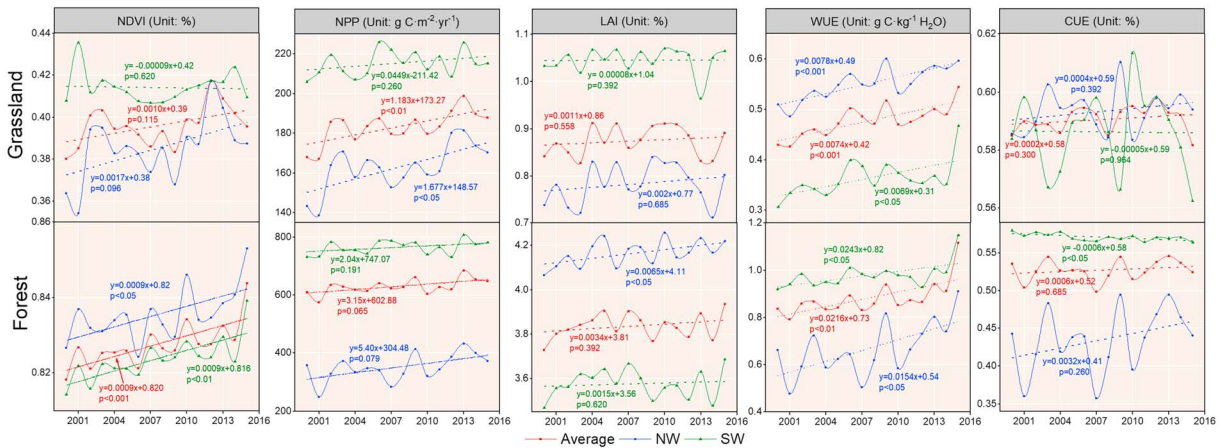


Figure 4. The temporal dynamics of NDVI, NPP, LAI, WUE, and CUE for forests and grasslands from 2000 to 2015. NDVI = normalized difference vegetation index; NPP = net primary productivity; LAI = leaf area index; WUE = water use efficiency; CUE = carbon use efficiency.

and croplands had previously occurred. By contrast, the conversion between forests and grasslands characterized in southwestern China. The areas with a transition from grasslands to forests were mainly scattered in Yunnan, and northwestern Guangxi. Regions transferred from forests to grasslands were generally concentrated in central of Sichuan, and eastern Guangxi. The transition from croplands to grasslands mainly occurred in central of Gansu, northern Shaanxi, and western Xinjiang. The conversion from croplands to forests mainly concentrated in northeastern Sichuan, and northern Chongqing.

3.2. Spatiotemporal Dynamics of NDVI, NPP, LAI, WUE, and CUE of Forests and Grasslands

The spatial and temporal dynamics of NDVI, NPP, LAI, WUE, and CUE of forests and grasslands in western, northwestern, and southwestern China were evaluated (Figure 4). The NDVI of forests and grasslands increased with a rate of 0.92% ($p < 0.001$) and 1.0% ($p = 0.115$) every 10 years over the past 16 years, respectively. The NDVI of forests increased significantly in both of northwestern ($p < 0.05$) and southwestern China ($p < 0.01$) during the 2000–2015 period. The temporal trend of averaged NDVI of grasslands exhibited an overall asymmetric “M” shape, peaking in 2012, and bottoming out in 2001. The NDVI of grasslands in northwestern China showed an overall increasing trend ($p = 0.096$), whereas NDVI decreased slightly throughout the entire study period in southwestern China ($p = 0.620$). The mean NPP of forests and grasslands both showed an overall increasing trend with rates of 31.49 ($p = 0.065$) and 11.83 ($p < 0.01$) $\text{g C}\cdot\text{m}^{-2}\cdot 10\text{ year}^{-1}$, respectively. The mean NPP of grasslands increased faster in northwestern region ($p < 0.05$) than in the southwest ($p = 0.260$). Similarly, the mean NPP of forests in northwestern region increased at a rate of 53.98 $\text{g C}\cdot\text{m}^{-2}\cdot 10\text{ year}^{-1}$ ($p = 0.079$), which was higher than that in southwestern region (20.36 $\text{g C}\cdot\text{m}^{-2}\cdot 10\text{ year}^{-1}$; $p = 0.191$). The LAI of grasslands increased with a rate of 1.13% every 10 years ($p = 0.558$) in western China during the 2000–2015 period. The LAI of grassland showed an overall increasing trend in northwestern region (2.02% every 10 years, $p = 0.685$). In contrast, the LAI of grassland in southwestern region kept nearly steady with a slightly increase (0.08% every 10 years, $p = 0.392$). The LAI of forests in western China increased at an average rate of 3.45% every 10 years ($p = 0.392$), and 1.47% ($p = 0.620$) and 6.51% every 10 years ($p < 0.05$) in northwestern region and southwestern region, respectively. The WUE of both grasslands and forests increased significantly during the entire study period, particularly with a vigorous increase in the last five years. For grasslands, WUE increased at a rate of 0.0074 ($p < 0.001$), 0.0078 ($p < 0.001$), and 0.0069 ($p < 0.05$) $\text{g C}\cdot\text{kg}^{-1}\text{ H}_2\text{O}\cdot\text{year}^{-1}$ in the western, northwestern, and southwestern regions of western China, respectively. The rate of increase of WUE of forests was higher than that of grasslands, which was 0.022 ($p < 0.01$), 0.015 ($p < 0.05$), and 0.024 ($p < 0.05$) $\text{g C}\cdot\text{kg}^{-1}\text{ H}_2\text{O}\cdot\text{year}^{-1}$ in the western, northwestern, and southwestern regions, respectively. The CUE of forests changed more dramatically than that of grasslands. The CUE of grasslands in western China increased slightly with a rate of 0.23% every 10 years ($p = 0.300$) over the past 16 years. The CUE of grasslands increased at a rate of 0.40% every 10 years in northwestern region ($p = 0.392$); however, it decreased by 0.05% every 10 years in southwestern region ($p = 0.964$). For the forests, CUE increased at a rate of 0.61% every 10 years in western China ($p = 0.685$). The CUE of

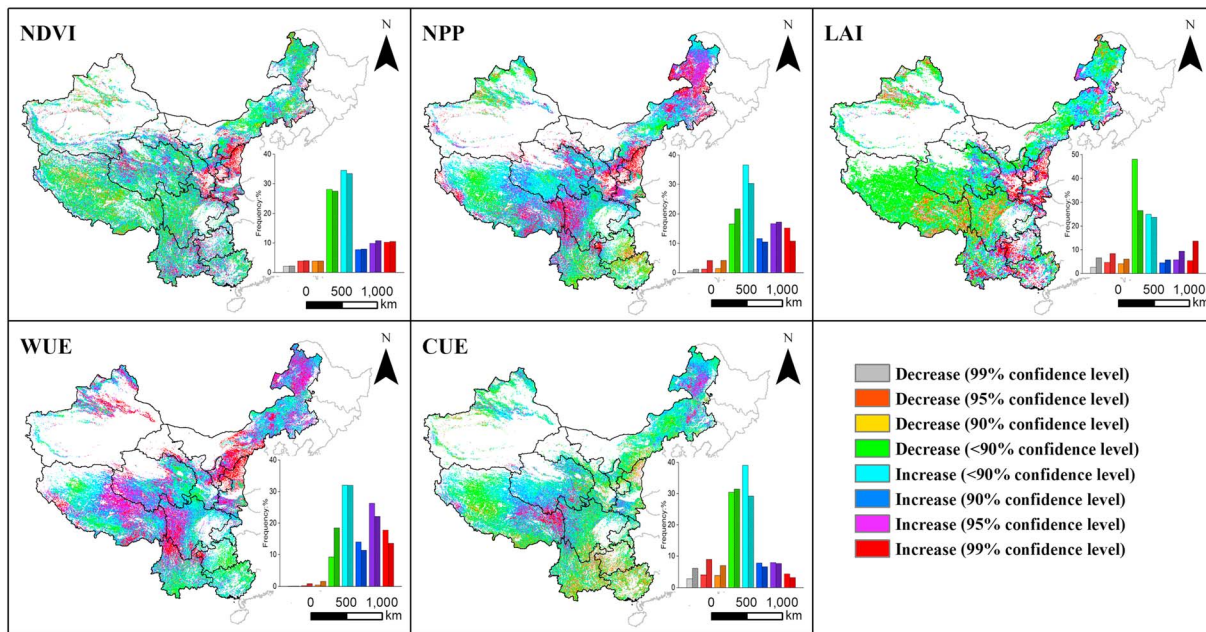


Figure 5. The spatial dynamics of NDVI, NPP, LAI, WUE, and CUE for forests and grasslands from 2000 to 2015. The plain bar indicates the frequency of grasslands, and the gridded bar represent the frequency of forests. NDVI = normalized difference vegetation index; NPP = net primary productivity; LAI = leaf area index; WUE = water use efficiency; CUE = carbon use efficiency.

forests presented an overall increasing trend at a rate of 3.23% every 10 years ($p = 0.260$), whereas it decreased significantly at a rate of 0.64% every 10 years in the southwest region ($p < 0.05$).

Spatially, regions of forests experiencing a significant increase in NDVI accounted for 21.25% of the total area of forests, and 20.05% of grassland regions exhibited a significant increase in NDVI (Figure 5). These regions were mainly concentrated in the Loess Plateau, southeastern Gansu, central of Qinghai, and in southern Sichuan basin. The NPP increased significantly in 28.01% and 31.94% of the total area of forests and grasslands, respectively, over the 16-year study period, which spanned northern Inner Mongolia, Shaanxi, Gansu, Qinghai, Sichuan, and Tibet. Regions exhibiting a significant increase in LAI accounted for 23.04% of the total area of forests, and 11.18% of the total area of grasslands. These regions were mainly located in Shaanxi, eastern Gansu, southern Sichuan Basin, and southwestern Yunnan. The spatial extent of regions presenting a significant increase of WUE included up to 35.68% and 44.02% of the total area of forests and grasslands, respectively. The spatial distributions of these regions showed a similar pattern to NPP and were mainly located in northern Xinjiang and Inner Mongolia, Shaanxi-Gansu-Ningxia regions, and the Three-River Source region. In contrast, 10.83% of forest CUE and 12.21% of grassland CUE increased significantly over the 16-year period, which mainly occurred in eastern Inner Mongolia and in the Three-River Source region. Uncertainty analysis indicated that all these indicators shared a generally similar pattern with lower uncertainty in arid and semiarid regions in northwestern China, but relatively higher uncertainty in humid regions in southwestern China, especially in eastern Inner Mongolia, Guizhou, Guangxi, and Yunnan (Figure 6).

3.3. Correlations Between Climate Factors and NDVI, NPP, LAI, WUE, and CUE of Forests and Grasslands

The correlations between climatic factors (temperature, precipitation, and solar radiation) and NDVI, NPP, LAI, WUE, and CUE of forests and grasslands were identified to reflect how the ongoing climatic factors affect these ecosystem functions (Figure 7). The results showed that, in principle, the precipitation was the primary climatic factor that affected these indicators in western China. Specifically, regions presenting a significantly positive correlation (at 95% and 99% confidence level) between grassland NDVI and precipitation accounted for 22.06% of total grasslands, which were mainly located in eastern Inner Mongolia, northern Loess Plateau, and central of Qinghai. In contrast, 2.97% and 3.34% of grassland regions showed

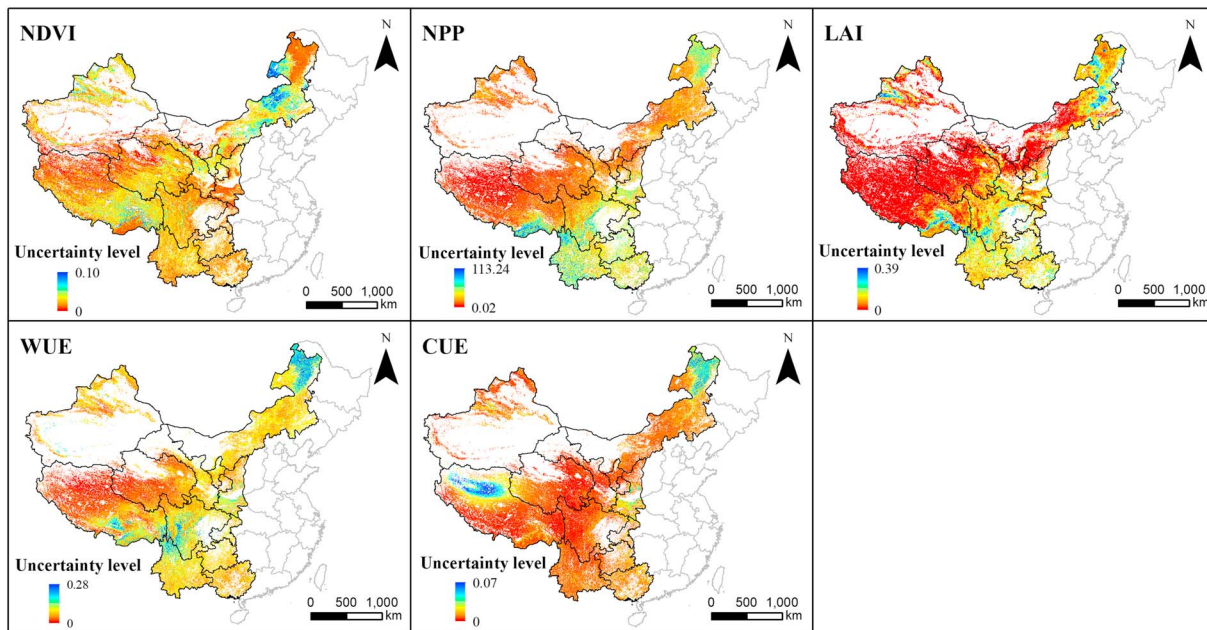


Figure 6. The uncertainty level for changes of NDVI, NPP, LAI, WUE, and CUE from 2000 to 2015. The uncertainty level was presented as the width of the confidence interval (i.e., differences between the upper and lower bounds) at 95% confidence level. NDVI = normalized difference vegetation index; NPP = net primary productivity; LAI = leaf area index; WUE = water use efficiency; CUE = carbon use efficiency.

a significantly positive correlation (at 95% and 99% confidence level) between NDVI with temperature and solar radiation, respectively. Similarly, regions showing a significantly positive correlation (at 95% and 99% confidence level) between grassland NPP and precipitation accounted for 23.70% of total grasslands. Most of these regions were located in eastern Inner Mongolia, extending to Gansu and Qinghai. However, only 4.46% and 4.45% of regions showed a significantly positive correlation (at 95% and 99% confidence level) between grassland NPP and both temperature and solar radiation. Regions showing a significantly positive correlation (at 95% and 99% confidence level) between grassland LAI with precipitation, temperature and radiation accounted for 16.56%, 1.26% and 2.42% of the total grasslands, respectively; this indicates that precipitation was also the leading climatic factor affecting the LAI of grasslands. The proportion of regions presenting a significantly positive correlation (at 95% and 99% confidence level) between grassland WUE and solar radiation was 9.72%, which was higher than that with precipitation and temperature (2.74% vs. 6.96%, respectively). Regions that showed a significantly positive correlation (at 95% and 99% confidence level) between grassland CUE with precipitation, temperature, and solar radiation took up to 5.12%, 4.64%, and 2.68% of total grasslands, respectively.

As for forests, precipitation was also the primary climatic factor affecting the functioning of forest ecosystems. Regions showing a significantly correlation (at 95% and 99% confidence level) between precipitation with NDVI, NPP, LAI, WUE, and CUE accounted for 12.15%, 23.75%, 11.73%, 26.00%, and 22.67% of the total forest area, respectively. These regions were mainly concentrated in the Greater Khingan Mountains in Inner Mongolia. Solar radiation was the second leading factor influencing these indicators. Regions presenting a significantly correlation (at 95% and 99% confidence level) between solar radiation with NDVI, NPP, LAI, WUE, and CUE accounted for 8.67%, 5.07%, 10.02%, 8.20%, and 9.90%, respectively. Meanwhile, regions showing a significantly correlations (at 95% and 99% confidence level) between temperature with NDVI, NPP, LAI, WUE, and CUE accounted for 7.14%, 6.70%, 6.21%, 7.64%, and 7.85% of the total forest land, respectively.

4. Discussion

4.1. Uncertainty of the Study

The land use and land cover types used in this study were derived from the ESA CCI product, which was developed based on Envisat MERIS, AVHRR, SPOT-VGT and PROBA-V data. These land cover maps

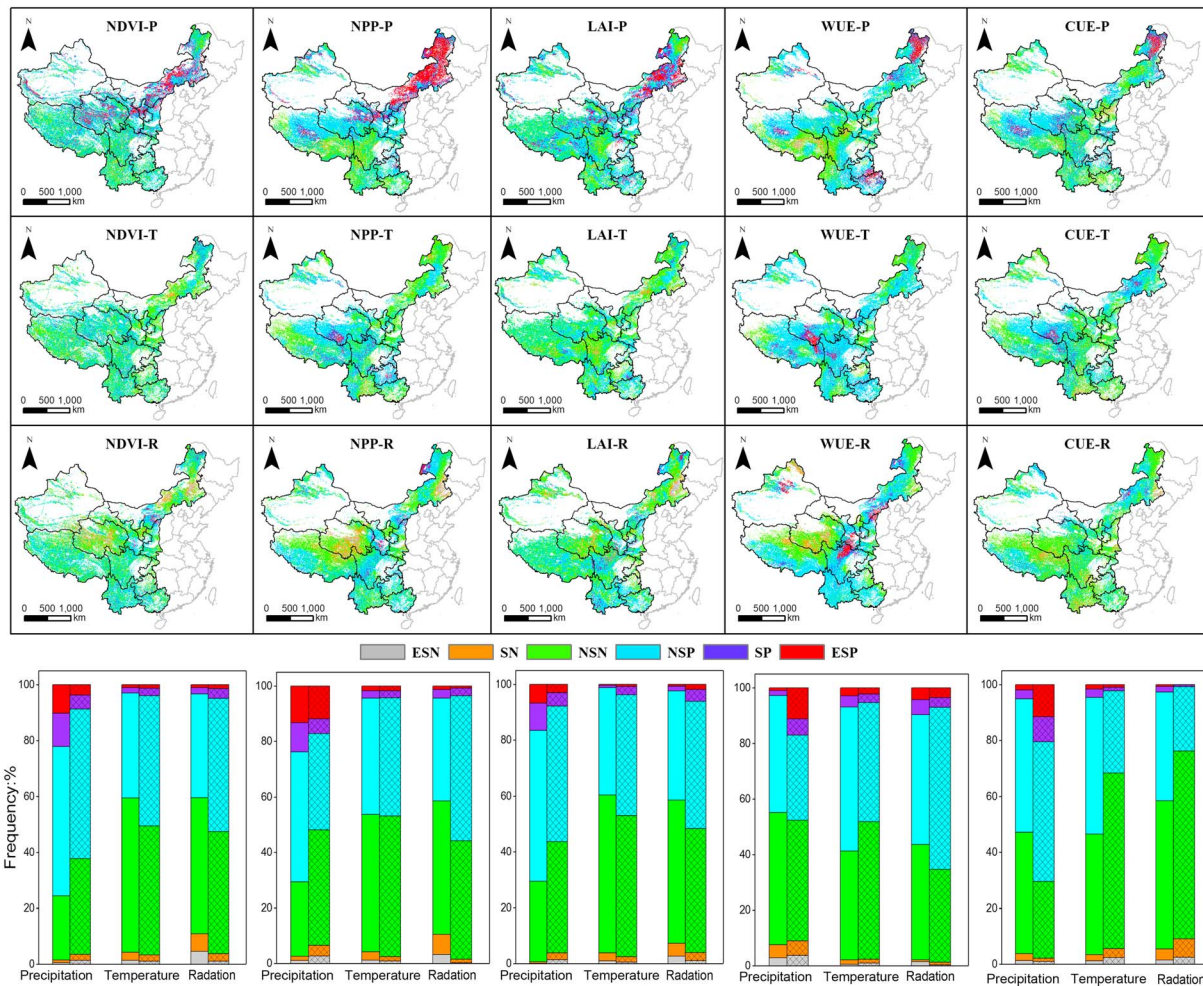


Figure 7. The spatial pattern of correlation coefficients between ecosystem functions (NDVI, NPP, LAI, WUE, and CUE) of forest and grassland with climate factors (MAT, MAP, and SR). The plain bar indicates the frequency of grasslands, and the gridded bar represent the frequency of forests. ESN = extremely significant negative correlation; SN = significant negative correlation; NSN = nonsignificant negative correlation; NS = nonsignificant positive correlation; S = significant positive correlation; E = Sextremely significant positive correlation; NDVI = normalized difference vegetation index; NPP = net primary productivity; LAI = leaf area index; WUE = water use efficiency; CUE = carbon use efficiency; MAT = mean annual temperature; MA = mean annual precipitation; SR = solar radiation.

have been validated against independent data including ground-based reference measurements and alternative estimates from other projects and sensors. The validation results showed that the croplands, forests, and grasslands all have accuracy values higher than 80%, whereas the classified area with mosaic classes of natural vegetation are identified with the lowest user accuracy values (Bontemps et al., 2015; ESA, 2017). The limitation of CCI maps lies in that not all changes between land use classes are captured, such as the conversion between forest classes. In addition, the changes detection methods need to allow the observation of a newly developed class during at least two consecutive years (Bontemps et al., 2013; ESA, 2017). The number of valid observations over western China used in the CCI-LC maps provides an indication of the classification reliability, which showed a higher level of reliability in northwestern China and a relatively lower level of reliability in southwestern China (Figure S2). In addition, the land use and land cover types in western China from multiple data sources were compared (Figure S3). The results demonstrated that the land cover maps based on ESA CCI-LC product showed higher consistency with the Landsat-based maps when compared with the MODIS data set, especially in northwestern China. Larger discrepancies were found in the croplands and forests in Guizhou and Guangxi, which were likely caused by the mosaic class of forests and croplands existing in these regions. Nonetheless, the ESA CCI-LC products provide valuable consecutive annual land

Table 2
Comparison of the Results of Present Study With Other Studies^a

Region	Sources of results	LAI change	NDVI change	NPP change (Unit: g C·m ⁻² ·year ⁻¹)
Loess Plateau	Others' results	0.110/year (2000–2013) ^b (Xiao, 2014)	0.080/10 years (2000–2013; Zhao et al., 2018)	99.12 (2000–2010; Zhang et al., 2016)
Three-River Source Region	This study	0.180/year	0.052/10 years	70.75
	Others' results	NA	0.012/10 years (2000–2011; X. Liu, Zhang, et al., 2014)	59.37 (2005–2012; Shao et al., 2017)
Qinghai-Tibet Plateau	This study		0.014/10 years	43.11
	Others' results	0–0.050/year (2001–2014; Gu et al., 2016)	0.040/10 years (1998–2012; Pang et al., 2017)	20.15 (2000–2012; Xu et al., 2016)
	This study	0.030/year	0.053/10 years	22.27

Note. NA = not available.

^aThe study period of present study is from 2000 to 2015. ^b(2000–2013) indicates that the study period is from 2000 to 2013.

use maps for evaluating the LUCC at regional and global scales with fine resolution and reliable accuracy (Li et al., 2018).

The uncertainty presented in the MODIS data is mainly a result of the degradation of earth observing sensors caused by being exposure to the solar and cosmic radiation (Lyapustin et al., 2014). In the present study, the MODIS C6 version data were used to derive the vegetation NDVI and NPP in western China. The current C6 version data have been further improved to provide the most reliable MODIS record in modeling global carbon and for the analysis of vegetation dynamics (Gang et al., 2018; Hilker et al., 2012). We compared our simulated results of the Loess Plateau, Three-River Source region and the Qinghai-Tibetan Plateau with the results of previous studies (Table 2). For the Loess Plateau, the increasing trends of LAI, NDVI, and NPP found in the present study agreed well with the findings of previous studies. The possible causes of the differences include the different data sources, models, and time periods. Zhang et al. (2016) simulated an increasing trend of vegetation NPP by 99.12 g C·m⁻²·year⁻¹ in the Loess Plateau during 2000–2010 by using the CASA model, which is higher than our results based on MODIS NPP. Similarly, simulated changes of NDVI and NPP for Three-River Resource region and the Qinghai-Tibet Plateau were consistent with the findings of other studies (Table 2), implying that the data set and methods used in the present study can generally capture the changes of vegetation in western China.

4.2. LUCC of Forests and Grasslands in Western China

The evidence based on remote sensing data supports the concept that the ecosystem quality over western China has substantially improved since the initiation of ecological restoration projects in the late 1990s. For the period from 2000 to 2015, land conversion analysis shows that the area of forests and grasslands both increased in western China. The most evident transition was the conversion from deserts/barren areas to grasslands in Inner Mongolia, Gansu, Qinghai, and Xinjiang. Previous research has demonstrated that the grasslands in Inner Mongolia experienced a net increase of 77,993 km² caused by the conversion from deserts and croplands to grasslands (Mu et al., 2013). The low and medium coverage rates of grasslands in the Mu Us sandy regions expanded from 2000 to 2010 (Karnieli et al., 2014; Li et al., 2017). Afforestation/reforestation and sowing of grasses are major techniques used in the GGP. According to year-book data, the area of manual afforestation and newly enclosed forests obviously increased in western China, particularly from 2000 to 2015 (Figure S4). Meanwhile, the areas of newly developed grasslands have also expanded in recent years (Figure S5). Fencing and enclosures were adopted in regions where heavily degraded grasslands were previously located, allowing the native grass species to become re-established, colonize, and succeed (Liu et al., 2004). Rotation grazing and seasonal enclosures provide superior methods of maintaining the grass community in slightly and moderately degraded regions (Gao & Liu, 2010). Cultivated pastures with intensive agronomic activity, such as sowing, irrigating, and fertilizing, has also been adopted in regions with variable terrain (Gang et al., 2018).

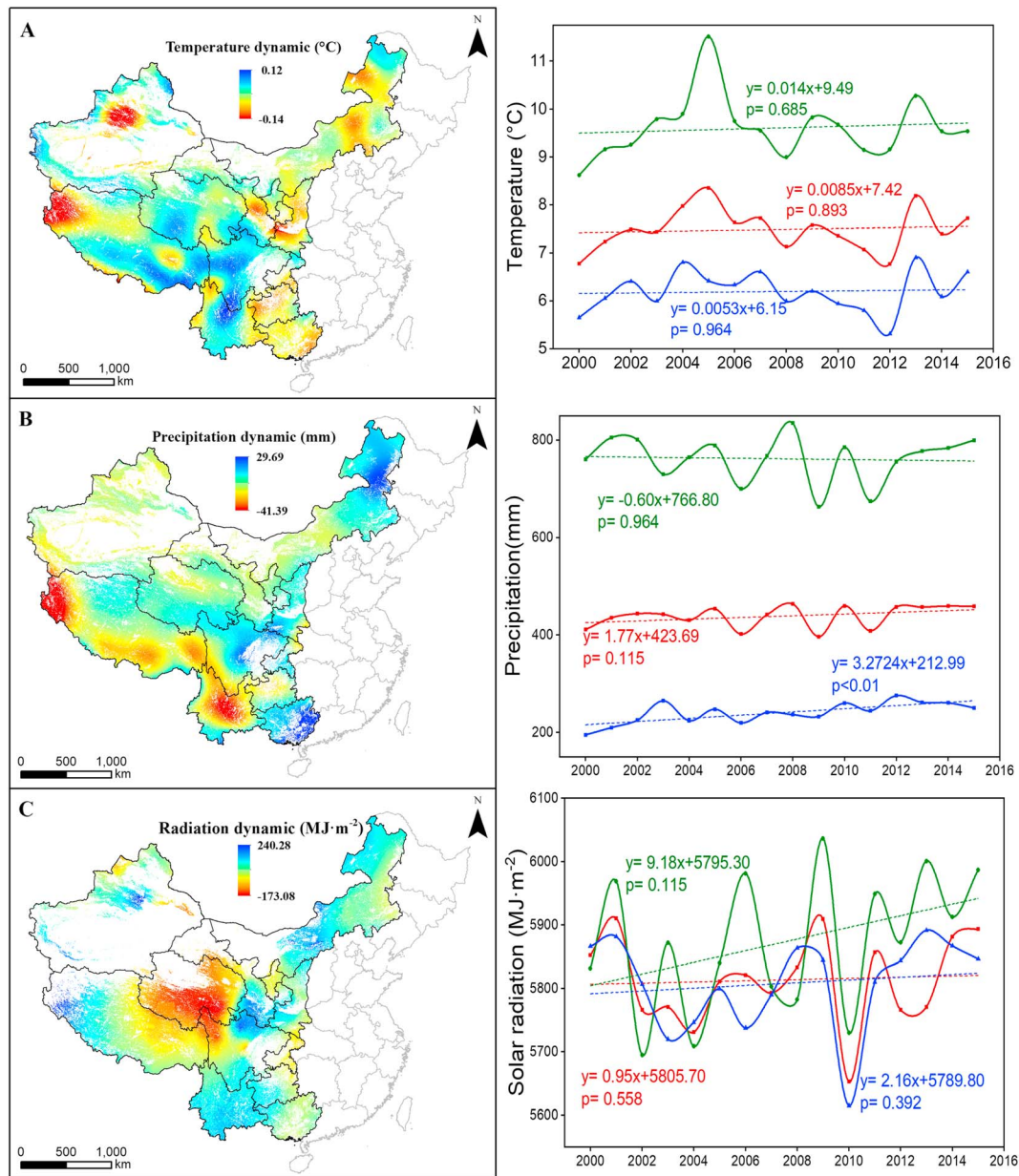


Figure 8. The spatial and temporal dynamics of MAT (a), MAP (b), and SR (c) during the 2000–2015 period. MAT = mean annual temperature; MAP = mean annual precipitation; SR = solar radiation. The green, blue, and red line represent the dynamic of averaged value in southwestern, northwestern, and western China, respectively.

4.3. Effects of Climate Factors and Human's Interference on Vegetation Recovery

Variations in climate have also benefited the recovery of vegetation on the landscape of western China to some extent. The spatial and temporal dynamics of MAT, MAP, and solar radiation during the 2000–2015 period are presented in Figure 8. MAT increased obviously in southwestern parts of the study area, such as eastern Tibet, western Sichuan, and northern Yunnan (Figure 8a). Meanwhile, regions that experienced increased MAP mainly located in Guangxi, Inner Mongolia, and Sichuan (Figure 8b). The temporal trends of MAP and MAT indicated that western China experienced a generally warmer and wetter trend from 2000–2015. In northwestern China, decreasing temperatures and increasing precipitation rates would cause a lower surface evaporation potential and higher soil moisture, thereby contributing to the growth of vegetation, such as in the Inner Mongolia, and Shaanxi-Gansu-Ningxia region. In contrast,

solar radiation or temperature would play a dominant factor in controlling plant growth in the rainfall-rich regions, such as southwestern China and on the Qinghai-Tibet Plateau (Piao et al., 2006; Sun & Zhu, 2001). The relationships between climate factors and NDVI, NPP, LAI, WUE, and CUE of forests and grasslands in northwestern and southwestern China were examined using statistical analysis, respectively (Figures S6 and S7). For northwestern China, the precipitation was significantly related with NDVI ($p < 0.001$), NPP ($p < 0.01$), and LAI ($p < 0.01$), implying that rising precipitation contribute to the increasing trend of NDVI, NPP, and LAI over the 16-year period. However, there were no significant relationships between temperature, solar radiation with NDVI, NPP, LAI, WUE, and CUE in northwestern China (Figure S6). For southwestern China, climate factors were not significantly related to with NDVI, NPP, LAI, WUE, and CUE of forests and grasslands (Figure S7). The greening trend and improved environment in southwestern China reflects the success of environmental restoration efforts, even under unfavorable climatic conditions (Brandt et al., 2018).

The functioning of ecosystems in western China have improved since the implementation of the ecological projects. An increasing trend in NDVI and NPP can be widely seen in the forest and grassland regions, especially in the Yellow River Basin. Previous studies have reported that ecological restoration efforts have caused an increase in the NDVI by more than 0.01 year^{-1} during the 2001–2010 period as a results of ecological restoration in Yulin and Yan'an prefectures in Shaanxi (Sun et al., 2015). The average tree cover substantially increased with a relative increase of 41.0% in the Loess Plateau from 2000 to 2010, and, as a result, the region has changed function from being a net carbon source into a net carbon sink (Feng et al., 2013; Xiao, 2014). Similar trend of change in NDVI or NPP have also been reported in Inner Mongolia (Mu et al., 2013; Zhang et al., 2015), Qinghai (L. Zhang, Guo, et al., 2014; Zhao et al., 2015), and Xinjiang (Yang et al., 2014). The largely land conversion of croplands and grasslands to forests under the GGP led to the increase of LAI (Xiao, 2014). The spatial and temporal trends of LAI based on GLOBMAP LAI product were also compared with the results of the Global Inventory Modeling and Mapping Studies (GIMMS) LAI v4.0 data set. The spatial pattern of LAI dynamic generated by GIMMS LAI agreed well with that of MODIS-based result, which mainly increased in Shaanxi-Gansu-Ningxia region, and the interwoven region of Guizhou, Gangxi, and Yunnan (Figure S8). In addition, the increasing trends of LAI for forests and grasslands in western China were also captured by the GIMMS LAI data set (Figure S8). The ET exhibited weak decreasing trends in northwestern ($p = 0.620$) and southwestern China ($p = 0.115$) over the 16-year period, which was caused by the meteorological factors as well as by the change of fractions of ET component, such as the less evaporation from soil (He et al., 2018; Zhang et al., 2016; Figure S9). Combing with the rising NPP, the WUE of grasslands and forests both increased over the 16-year period, which are beneficial effects of the GGP. The previous study showed that the WUE in the Loess Plateau increased at a rate of $0.027 \text{ g C/kg H}_2\text{O}$ during the period 2000–2010, which is higher than our simulation ($0.020 \text{ g C/kg H}_2\text{O}$; Zhang et al., 2016). This is probably caused by the faster increasing trend of NPP simulated by CASA model. Management activities, such as the reduction in grazing during afforestation/reforestation, fencing of some areas, and grazing prohibition in general currently serve as effective ways to increase vegetation biomass and reverse environment degradation. Furthermore, the traditional method used to feed grazing animals has shifted from open grazing to the use of feedlots, with the goal of preventing the excessive removal and loss of vegetation caused by unsustainable stocking rates for livestock (Cheng et al., 1995).

The current research mainly focused on the aboveground biophysical characteristics of vegetation, and evidences have demonstrated that the soil properties have also improved substantially during the process of vegetation recovery (Deng et al., 2014, 2017; D. Liu, Chen, et al., 2014). The increased carbon sequestration of vegetation compensates for the carbon loss caused by deforestation or land conversion (Brandt et al., 2018; Tian et al., 2011). However, the monoculture plantations of the GGP have been criticized for providing poor habitats for native species, and for being highly vulnerable to natural disturbances, such as drought, diseases, and pests (Cao et al., 2011; Delang & Yuan, 2015). In addition, some researchers have warned that the NPP of vegetation is approaching the limit of available and sustainable water resources in the currently re-vegetated regions, and increased human demands for water resources complicates environmental concerns in the Loess Plateau (Feng et al., 2016). Therefore, local socioeconomic related problems should not be neglected (Brandt et al., 2018; Cao et al., 2011, 2017).

5. Conclusions

An analysis of various remote sensing-based ecological indicators showed that the GGP has significantly improved the functioning of forest and grassland ecosystems in western China. Despite a small decrease that occurred in the spatial extent of grasslands in southwestern region, the total spatial extent of forests and grasslands expanded from 2000 to 2015 in western China. The transition from deserts to grasslands in northwestern China was the prominent feature during the 16-year period analyzed here. During the study period, grassland NPP and WUE, as well as forest NDVI and WUE, increased significantly. The LAI and CUE of forests and grasslands also showed an overall increasing trend. These indicators showed asymmetric responses in the southwest and northwest regions of western China. Despite the fact that increased precipitation has beneficial effects for the vegetation recovery in some regions, the GGP was the dominant factor leading to the improvement of ecosystem function in the entire regions of western China, especially in the Loess Plateau and Three-River Source regions. Nonetheless, a reasonable planting strategy still needs to be developed to resolve socioeconomic and environmental sustainability issues as well as to balance the trade-off between grain production and greening of the environment. Due to the limited data availability and method constraints, only the changes of vegetation NDVI, NPP, LAI, WUE, and CUE during the period 2000–2015 in western China were quantified. In addition, factors such as CO₂ concentrations and irrigated water supplies were not considered in the present study, which also play important roles in the ecosystem functions response. Longer-term of remote sensing monitoring coupled with land-atmosphere models are needed to provide a more comprehensive picture of the net effects of the GGP in western China in further research.

Conflicts of Interest

None declared.

Acknowledgments

This work was supported by the National Natural Science Foundation of China (grant 31602004), the National Key Research and Development Program of China (grant 2016YFC0501707), the CAS “Light of West China” program (grant XAB2016B05), the Special Foundation for State Basic Research Program of China (grant 2014YF210100), the Key Cultivation Project of Chinese Academy of Sciences “The promotion and management of ecosystem functions of restored vegetation in Loess Plateau, China,” and the Fundamental Research Funds for the Central Universities (grant 2452017184). We thank Prof. Hanqin Tian for his guidance on this paper. We also appreciate the China Meteorological Data Service Center, the ESA CCI Land Cover project, and the NTSG for sharing data set. All the data used in the paper are publicly accessed through the website provided in the main text.

References

- Andersson, E., Brogaard, S., & Olsson, L. (2011). The political ecology of land degradation. In A. Gadgil & D. M. Liverman (Eds.), *Annual Review of Environment and Resources* (pp. 295–319). Palo Alto: Annual Reviews.
- Bai, Z. G., Dent, D. L., Olsson, L., & Schaepman, M. E. (2008). Proxy global assessment of land degradation. *Soil Use and Management*, 24(3), 223–234. <https://doi.org/10.1111/j.1475-2743.2008.00169.x>
- Barrow, C. J. (1991). *Land degradation: Development and breakdown of terrestrial environments*. Cambridge: Cambridge University Press.
- Beer, C., Reichstein, M., Tomelleri, E., Ciais, P., Jung, M., Carvalhais, N., et al. (2010). Terrestrial gross carbon dioxide uptake: Global distribution and covariation with climate. *Science*, 329(5993), 834–838. <https://doi.org/10.1126/science.1184984>
- Bontemps, S., Boettcher, M., Brockmann, C., Kirches, G., Lamarche, C., Radoux, J., et al. (2015). Multi-year global land cover mapping at 300 m and characterization for climate modelling: Achievements of the land cover component of the ESA Climate Change Initiative, paper presented at The International Archives of Photogrammetry, Remote Sensing and Spatial Information Sciences, 323–328.
- Bontemps, S., Defourny, P., Radoux, J., Van Bogaert, E., Lamarche, C., Achard, F., et al. (2013). Consistent global land cover maps for climate modelling communities: Current achievements of the ESA's land cover CCI, paper presented at Proceedings of the ESA Living Planet Symposium, Edinburgh, 9–13.
- Brandt, M., Yue, Y., Wigneron, J. P., Tong, X., Tian, F., Jepsen, M. R., et al. (2018). Satellite-observed major greening and biomass increase in south China karst during recent decade. *Earth's Future*, 6(7), 1017–1028. <https://doi.org/10.1029/2018EF000890>
- Cao, S., Chen, L., Shankman, D., Wang, C., Wang, X., & Zhang, H. (2011). Excessive reliance on afforestation in China's arid and semi-arid regions: Lessons in ecological restoration. *Earth-Science Reviews*, 104(4), 240–245. <https://doi.org/10.1016/j.earscirev.2010.11.002>
- Cao, S., Shang, D., Yue, H., & Ma, H. (2017). A win-win strategy for ecological restoration and biodiversity conservation in Southern China. *Environmental Research Letters*, 12(4), 44004. <https://doi.org/10.1088/1748-9326/aa650c>
- Chen, Y., Wang, K., Lin, Y., Shi, W., Song, Y., & He, X. (2015). Balancing green and grain trade. *Nature Geoscience*, 8(10), 739–741. <https://doi.org/10.1038/ngeo2544>
- Cheng, J., Zou, H., & Akio, H. (1995). The rational utilization of grassland and successional course of grassland vegetation in the Loess Plateau. *Acta Pratacultura Sinica*, 4, 17–22.
- Delang, C. O., & Yuan, Z. (2015). *China's Grain for Green Program*. Cham: Springer International. <https://doi.org/10.1007/978-3-319-11505-4>
- Deng, F., Chen, J. M., Plummer, S., Chen, M., & Pisek, J. (2006). Algorithm for global leaf area index retrieval using satellite imagery. *IEEE Transactions On Geoscience and Remote Sensing*, 44(8), 2219–2229. <https://doi.org/10.1109/TGRS.2006.872100>
- Deng, L., Liu, G. B., & Shangguan, Z. P. (2014). Land-use conversion and changing soil carbon stocks in China's 'Grain-for-Green' Program: A synthesis. *Global Change Biology*, 20(11), 3544–3556. <https://doi.org/10.1111/gcb.12508>
- Deng, L., Liu, S., Kim, D. G., Peng, C., Sweeney, S., & Shangguan, Z. (2017). Past and future carbon sequestration benefits of China's Grain for Green Program. *Global Environmental Change*, 47, 13–20. <https://doi.org/10.1016/j.gloenvcha.2017.09.006>
- Dillaway, D. N., & Kruger, E. L. (2014). Trends in seedling growth and carbon-use efficiency vary among broadleaf tree species along a latitudinal transect in eastern North America. *Global Change Biology*, 20(3), 908–922. <https://doi.org/10.1111/gcb.12427>
- Ding, Y., & Dong, G. (2002). *Assessment of environmental evolution of western China: Environmental characteristics and evolution of western China*. Beijing: Science Press.
- Duveiller, G., Hooker, J., & Cescatti, A. (2018). A dataset mapping the potential biophysical effects of vegetation cover change. *Scientific Data*, 5, 180014. <https://doi.org/10.1038/sdata.2018.14>

- ESA (2017). ESA: Land cover CCI product user guide version 2.0. Retrieved from http://maps.elie.ucl.ac.be/CCI/viewer/download/ESACCI-LC-Ph2-PUGv2_2.0.pdf
- Feng, X., Fu, B., Lu, N., Zeng, Y., & Wu, B. (2013). How ecological restoration alters ecosystem services: An analysis of carbon sequestration in China's Loess Plateau. *Scientific Reports*, 3(1), 2846. <https://doi.org/10.1038/srep02846>
- Feng, X., Fu, B., Piao, S., Wang, S., Ciais, P., Zeng, Z., et al. (2016). Revegetation in China's Loess Plateau is approaching sustainable water resource limits. *Nature Climate Change*, 6(11), 1019–1022. <https://doi.org/10.1038/NCLIMATE3092>
- Gang, C., Wang, Z., Chen, Y., Yang, Y., Li, J., Cheng, J., et al. (2016). Drought-induced dynamics of carbon and water use efficiency of global grasslands from 2000 to 2011. *Ecological Indicators*, 67, 788–797. <https://doi.org/10.1016/j.ecolind.2016.03.049>
- Gang, C., Zhao, W., Zhao, T., Zhang, Y., Gao, X., & Wen, Z. (2018). The impacts of land conversion and management measures on the grassland net primary productivity over the Loess Plateau, Northern China. *Science of the Total Environment*, 645, 827–836. <https://doi.org/10.1016/j.scitotenv.2018.07.161>
- Gao, J., & Liu, Y. (2010). Determination of land degradation causes in Tongyu County, Northeast China via land cover change detection. *International Journal of Applied Earth Observation and Geoinformation*, 12(1), 9–16. <https://doi.org/10.1016/j.jag.2009.08.003>
- Gibbs, H. K., & Salmon, J. M. (2015). Mapping the world's degraded lands. *Applied Geography*, 57, 12–21. <https://doi.org/10.1016/j.apgeog.2014.11.024>
- Gu, X., Li, M., Xu, D., Zhang, B., Nie, X., Li, H., et al. (2016). *Green book of remote sensing monitoring: Report on remote sensing monitoring of China sustainable development*. Beijing: Social Sciences Academic press.
- He, L., Chen, J. M., Gonsamo, A., Luo, X., Wang, R., Liu, Y., & Liu, R. (2018). Changes in the shadow: The shifting role of shaded leaves in global carbon and water cycles under climate change. *Geophysical Research Letters*, 45, 5052–5061. <https://doi.org/10.1029/2018GL077560>
- Hilker, T., Lyapustin, A. I., Tucker, C. J., Sellers, P. J., Hall, F. G., & Wang, Y. (2012). Remote sensing of tropical ecosystems: Atmospheric correction and cloud masking matter. *Remote Sensing of Environment*, 127, 370–384. <https://doi.org/10.1016/j.rse.2012.08.035>
- Karnieli, A., Qin, Z., Wu, B., Panov, N., & Yan, F. (2014). Spatio-temporal dynamics of land-use and land-cover in the Mu Us Sandy Land, China, using the change vector analysis technique. *Remote Sensing*, 6(10), 9316–9339. <https://doi.org/10.3390/rs6109316>
- Kendall, M. G. (1948). *Rank correlation methods*. London: Griffin. <https://doi.org/10.2307/2333282>
- Kuppel, S., Fan, Y., & Jobbágy, E. G. (2017). Seasonal hydrologic buffer on continents: Patterns, drivers and ecological benefits. *Advances in Water Resources*, 102, 178–187. <https://doi.org/10.1016/j.advwatres.2017.01.004>
- Le, Q., Nkonya, E., & Mirzabaev, A. (2016). Biomass productivity-based mapping of global land degradation hotspots. In *Economics of land degradation and improvement—A global assessment for sustainable development* (pp. 55–84). Cham: Springer. https://doi.org/10.1007/978-3-319-19168-3_4
- Li, W. (2000). Several problems of eco-environment construction in the southwestern China. *Scientia Silvae Sinicae*, 10–11.
- Li, W., MacBean, N., Ciais, P., Defourny, P., Lamarche, C., Bontemps, S., et al. (2018). Gross and net land cover changes in the main plant functional types derived from the annual ESA CCIz land cover maps (1992–2015). *Earth System Science Data*, 10(1), 219–234. <https://doi.org/10.5194/essd-10-219-2018>
- Li, Y., Cao, Z., Long, H., Liu, Y., & Li, W. (2017). Dynamic analysis of ecological environment combined with land cover and NDVI changes and implications for sustainable urban-rural development: The case of Mu Us Sandy Land, China. *Journal of Cleaner Production*, 142, 697–715. <https://doi.org/10.1016/j.jclepro.2016.09.011>
- Liang, W., Yang, Y., Fan, D., Guan, H., Zhang, T., Long, D., et al. (2015). Analysis of spatial and temporal patterns of net primary production and their climate controls in China from 1982 to 2010. *Agricultural and Forest Meteorology*, 204, 22–36. <https://doi.org/10.1016/j.agrformet.2015.01.015>
- Liu, D., Chen, Y., Cai, W., Dong, W., Xiao, J., Chen, J., et al. (2014). The contribution of China's Grain to Green Program to carbon sequestration. *Landscape Ecology*, 29(10), 1675–1688. <https://doi.org/10.1007/s10980-014-0081-4>
- Liu, G., & Lu, X. (2009). Research progress of climatic change in western China on the background of global warming. *Meteorological and Environmental Sciences*, 32, 69–73.
- Liu, M., Jiang, G., Li, L., Li, Y., Gao, L., & Niu, S. (2004). Control of sandstorms in inner Mongolia, China. *Environmental Conservation*, 31(4), 269–273. <https://doi.org/10.1017/S0376892904001675>
- Liu, X., Zhang, J., Zhu, X., Pan, Y., Liu, Y., Zhang, D., & Lin, Z. (2014). Spatiotemporal changes in vegetation coverage and its driving factors in the Three-River Headwaters Region during 2000–2011. *Journal of Geographical Sciences*, 24(2), 288–302. <https://doi.org/10.1007/s11442-014-1088-0>
- Liu, X., Zhu, X., Pan, Y., Li, S., Ma, Y., & Nie, J. (2016). Vegetation dynamics in Qinling-Daba Mountains in relation to climate factors between 2000 and 2014. *Journal of Geographical Sciences*, 26(1), 45–58. <https://doi.org/10.1007/s11442-016-1253-8>
- Liu, Y., Liu, R., & Chen, J. M. (2012). Retrospective retrieval of long-term consistent global leaf area index (1981–2011) from combined AVHRR and MODIS data. *Journal of Geophysical Research*, 117, G04003. <https://doi.org/10.1029/2012JG002084>
- Lü, Y., Zhang, L., Feng, X., Zeng, Y., Fu, B., Yao, X., et al. (2015). Recent ecological transitions in China: Greening, browning, and influential factors. *Scientific Reports*, 5(1), 8732. <https://doi.org/10.1038/srep08732>
- Lyapustin, A., Tucker, J., Hall, F., Sellers, P., Wu, A., Angal, A., et al. (2014). Scientific impact of MODIS C5 calibration degradation and C6+ improvements. *Atmospheric Measurement Techniques*, 7(12), 4353–4365. <https://doi.org/10.5194/amt-7-4353-2014>
- Mann, H. B. (1945). Nonparametric tests against trend. *Econometrica: Journal of the Econometric Society*, 13(3), 245–259. <https://doi.org/10.2307/1907187>
- Monteith, J. L. (1972). Solar radiation and productivity in tropical ecosystems. *Journal of Applied Ecology*, 9(3), 747–766. <https://doi.org/10.2307/2401901>
- Moore, J. C., Chen, Y., Cui, X., Yuan, W., Dong, W., Gao, Y., & Shi, P. (2016). Will China be the first to initiate climate engineering? *Earths Future*, 4(12), 588–595. <https://doi.org/10.1002/2016EF000402>
- Mu, Q., Heinsch, F. A., Zhao, M., & Running, S. W. (2007). Development of a global evapotranspiration algorithm based on MODIS and global meteorology data. *Remote Sensing of Environment*, 111(4), 519–536. <https://doi.org/10.1016/j.rse.2007.04.015>
- Mu, Q., Zhao, M., & Running, S. W. (2011). Improvements to a MODIS global terrestrial evapotranspiration algorithm. *Remote Sensing of Environment*, 115(8), 1781–1800. <https://doi.org/10.1016/j.rse.2011.02.019>
- Mu, S., Zhou, S., Chen, Y., Li, J., Ju, W., & Odeh, I. O. A. (2013). Assessing the impact of restoration-induced land conversion and management alternatives on net primary productivity in Inner Mongolian grassland, China. *Global and Planetary Change*, 108, 29–41. <https://doi.org/10.1016/j.gloplacha.2013.06.007>

- Myneni, R. B., Hoffman, S., Knyazikhin, Y., Privette, J. L., Glassy, J., Tian, Y., et al. (2002). Global products of vegetation leaf area and fraction absorbed PAR from year one of MODIS data. *Remote Sensing of Environment*, 83(1-2), 214–231. [https://doi.org/10.1016/S0034-4257\(02\)00074-3](https://doi.org/10.1016/S0034-4257(02)00074-3)
- Pang, G., Wang, X., & Yang, M. (2017). Using the NDVI to identify variations in, and responses of, vegetation to climate change on the Tibetan Plateau from 1982 to 2012. *Quaternary International*, 444, 87–96. <https://doi.org/10.1016/j.quaint.2016.08.038>
- Peng, S., Piao, S., Ciais, P., Myneni, R. B., Chen, A., Chevallier, F., et al. (2013). Asymmetric effects of daytime and night-time warming on Northern Hemisphere vegetation. *Nature*, 501(7465), 88–92. <https://doi.org/10.1038/nature12434>
- Piao, S., Fang, J., & He, J. (2006). Variations in vegetation net primary production in the Qinghai-Xizang Plateau, China, from 1982 to 1999. *Climatic Change*, 74(1-3), 253–267. <https://doi.org/10.1007/s10584-005-6339-8>
- Piao, S., Fang, J., Liu, H., & Zhu, B. (2005). NDVI-indicated decline in desertification in China in the past two decades. *Geophysical Research Letters*, 32, L06402. <https://doi.org/10.1029/2004GL021764>
- Running, S. W., Nemani, R. R., Heinsch, F. A., Zhao, M. S., Reeves, M., & Hashimoto, H. (2004). A continuous satellite-derived measure of global terrestrial primary production. *Bioscience*, 54(6), 547–560. [https://doi.org/10.1641/0006-3568\(2004\)054\[0547:ACSMOG\]2.0.CO;2](https://doi.org/10.1641/0006-3568(2004)054[0547:ACSMOG]2.0.CO;2)
- Shao, Q., Cao, W., Fan, J., Huang, L., & Xu, X. (2017). Effects of an ecological conservation and restoration project in the Three-River Source Region, China. *Journal of Geographical Sciences*, 27(2), 183–204. <https://doi.org/10.1007/s11442-017-1371-y>
- Shi, Y., Shen, Y., Kang, E., Li, D., Ding, Y., Zhang, G., & Hu, R. (2007). Recent and future climate change in northwest China. *Climatic Change*, 80(3-4), 379–393. <https://doi.org/10.1007/s10584-006-9121-7>
- Sun, R., & Zhu, Q. (2001). Estimation of net primary productivity in China using remote sensing data. *Journal of Geographical Sciences*, 11(1), 14–23. <https://doi.org/10.1007/BF02837372>
- Sun, W., Song, X., Mu, X., Gao, P., Wang, F., & Zhao, G. (2015). Spatiotemporal vegetation cover variations associated with climate change and ecological restoration in the Loess Plateau. *Agricultural and Forest Meteorology*, 209–210, 87–99. <https://doi.org/10.1016/j.agrformet.2015.05.002>
- Taddese, G. (2001). Land degradation: A challenge to Ethiopia. *Environmental Management*, 27(6), 815–824. <https://doi.org/10.1007/s002670010190>
- Tessema, Z. K., de Boer, W. F., Rmt, B., & Hht, P. (2011). Changes in soil nutrients, vegetation structure and herbaceous biomass in response to grazing in a semi-arid savanna of Ethiopia. *Journal of Arid Environments*, 75(7), 662–670. <https://doi.org/10.1016/j.jaridenv.2011.02.004>
- Tian, H., Melillo, J., Lu, C., Kicklighter, D., Liu, M., Ren, W., et al. (2011). China's terrestrial carbon balance: Contributions from multiple global change factors. *Global Biogeochemical Cycles*, 25, GB1007. <https://doi.org/10.1029/2010GB003838>
- Tong, X., Wang, K., Yue, Y., Brandt, M., Liu, B., Zhang, C., et al. (2017). Quantifying the effectiveness of ecological restoration projects on long-term vegetation dynamics in the karst regions of southwest China. *International Journal of Applied Earth Observation and Geoinformation*, 54, 105–113. <https://doi.org/10.1016/j.jag.2016.09.013>
- Wang, X., Lu, C., Fang, J., & Shen, Y. (2007). Implications for development of grain-for-green policy based on cropland suitability evaluation in desertification-affected north China. *Land Use Policy*, 24(2), 417–424. <https://doi.org/10.1016/j.landusepol.2006.05.005>
- Xiao, J. (2014). Satellite evidence for significant biophysical consequences of the “Grain for Green” Program on the Loess Plateau in China. *Journal of Geophysical Research: Biogeosciences*, 119, 2261–2275. <https://doi.org/10.1002/2014JG002820>
- Xiao, J., & Moody, A. (2004). Trends in vegetation activity and their climatic correlates: China 1982 to 1998. *International Journal of Remote Sensing*, 25(24), 5669–5689. <https://doi.org/10.1080/01431160410001735094>
- Xu, H., Wang, X., & Zhang, X. (2016). Alpine grasslands response to climatic factors and anthropogenic activities on the Tibetan Plateau from 2000 to 2012. *Ecological Engineering*, 92, 251–259. <https://doi.org/10.1016/j.ecoleng.2016.04.005>
- Xu, Z. X., Chen, Y. N., & Li, J. Y. (2004). Impact of climate change on water resources in the Tarim River Basin. *Water Resources Management*, 18(5), 439–458. <https://doi.org/10.1023/B:WARM.0000049142.95583.98>
- Yang, H., Mu, S., & Li, J. (2014). Effects of ecological restoration projects on land use and land cover change and its influences on territorial NPP in Xinjiang, China. *Catena*, 115, 85–95. <https://doi.org/10.1016/j.catena.2013.11.020>
- Yang, Y., Xiao, P., Feng, X., & Li, H. (2017). Accuracy assessment of seven global land cover datasets over China. *ISPRS Journal of Photogrammetry & Remote Sensing*, 125, 156–173. <https://doi.org/10.1016/j.isprsjprs.2017.01.016>
- Yuan, W., Li, X., Liang, S., Cui, X., Dong, W., Liu, S., et al. (2014). Characterization of locations and extents of afforestation from the Grain for Green Project in China. *Remote Sensing Letters*, 5(3), 221–229. <https://doi.org/10.1080/2150704X.2014.894655>
- Yue, S., & Wang, C. Y. (2002). Applicability of prewhitening to eliminate the influence of serial correlation on the Mann-Kendall test. *Water Resources Research*, 38(6), 1068. <https://doi.org/10.1029/2001WR000861>
- Zhang, J., Huang, Y., Chen, H., Gong, J., Qi, Y., & Yang, F. (2015). Effects of grassland management on the community structure, above-ground biomass and stability of a temperate steppe in Inner Mongolia, China. *Journal of Arid Land*, 8(3), 422–433. <https://doi.org/10.1007/s40333-016-0002-2>
- Zhang, L., Guo, H., Wang, C., Ji, L., Li, J., Wang, K., & Dai, L. (2014). The long-term trends (1982–2006) in vegetation greenness of the alpine ecosystem in the Qinghai-Tibetan Plateau. *Environmental Earth Sciences*, 72(6), 1827–1841. <https://doi.org/10.1007/s12665-014-3092-1>
- Zhang, T., Peng, J., Liang, W., Yang, Y., & Liu, Y. (2016). Spatial-temporal patterns of water use efficiency and climate controls in China's Loess Plateau during 2000–2010. *Science of the Total Environment*, 565, 105–122. <https://doi.org/10.1016/j.scitotenv.2016.04.126>
- Zhang, X., & Liu, W. (2005). Simulating potential response of hydrology, soil erosion, and crop productivity to climate change in Changwu tableland region on the Loess Plateau of China. *Agricultural and Forest Meteorology*, 131(3-4), 127–142. <https://doi.org/10.1016/j.agrformet.2005.05.005>
- Zhang, Y., Yu, G., Yang, J., Wimberly, M. C., Zhang, X., Tao, J., et al. (2014). Climate-driven global changes in carbon use efficiency. *Global Ecology and Biogeography*, 23(2), 144–155. <https://doi.org/10.1111/geb.12086>
- Zhao, A., Zhang, A., Liu, X., & Cao, S. (2018). Spatiotemporal changes of normalized difference vegetation index (NDVI) and response to climate extremes and ecological restoration in the Loess Plateau, China. *Theoretical and Applied Climatology*, 132(1-2), 555–567. <https://doi.org/10.1007/s00704-017-2107-8>
- Zhao, G., Mu, X., Wen, Z., Wang, F., & Gao, P. (2013). Soil erosion, conservation, and eco-environment changes in the loess plateau of China. *Land Degradation & Development*, 24, 499–510. <https://doi.org/10.1002/ldr.2246>
- Zhao, H., Liu, S., Dong, S., Su, X., Wang, X., Wu, X., et al. (2015). Analysis of vegetation change associated with human disturbance using MODIS data on the rangelands of the Qinghai-Tibet Plateau. *The Rangeland Journal*, 37(1), 77–87. <https://doi.org/10.1071/RJ14061>
- Zhao, M., Heinsch, F. A., Nemani, R. R., & Running, S. W. (2005). Improvements of the MODIS terrestrial gross and net primary production global data set. *Remote Sensing of Environment*, 95(2), 164–176. <https://doi.org/10.1016/j.rse.2004.12.011>

- Zhao, M., Running, S. W., & Nemani, R. R. (2006). Sensitivity of Moderate Resolution Imaging Spectroradiometer (MODIS) terrestrial primary production to the accuracy of meteorological reanalyses. *Journal of Geophysical Research*, *111*, G01002. <https://doi.org/10.1029/2004JG000004>
- Zhou, H., & Van Rompaey, A. (2009). Detecting the impact of the “Grain for Green” program on the mean annual vegetation cover in the Shaanxi province, China using SPOT-VGT NDVI data. *Land Use Policy*, *26*(4), 954–960. <https://doi.org/10.1016/j.landusepol.2008.11.006>